A Software Tool for the Evaluation of the Behaviour of Bioelectrical Currents

Gianluca FABBRI, António João MARQUES CARDOSO
Department of Electrical and Computer Engineering – University of Coimbra, FCTUC/IT
Pólo II – Pinhal de Marrocos, P – 3030–290, Coimbra, Portugal
gianluca.fabbri@co.it.pt, acardoso@deec.uc.pt

and

Chiara BOCCALETTI
Department of Electrical Engineering – "Sapienza" University of Rome
Via Eudossiana 18, 00184, Rome, Italy
chiara.boccaletti@uniroma1.it

and

Luigi CASTRICA
Biophysics Research srl – Via di Quarto Rubbie 45, 00118, Rome, Italy

ABSTRACT

A software tool has been developed in order to evaluate bioelectrical currents. The tool is able to provide a graphical representation of the behaviour of small currents emitted by characteristic points of the human body and captured through a non invasive probe previously developed. The software implementation combines a variety of graphical techniques to create a powerful system that will enable users to perform an accurate and reliable analysis of the emitted currents and to easily go on to further applications and research. This paper introduces the design and the main characteristics of the tool and shows significant measurement results.

Keywords: Graphical User Interface, Biosensors, Noninvasive Measurements, Biopotential Electrodes, Bioelectrical Currents, Measurement and Instrumentation.

1. INTRODUCTION

Particular skin points of the human body are characterized by having a very low impedance. It has been shown that more than 90% of particularly low impedance skin points coincide with traditional Chinese Medicine acupuncture points [1]-[3]. The bioelectric properties of acupuncture points are not clearly understood yet but it is by now generally accepted that both meridians and acupuncture points have lower electrical resistance or impedance than nearby surrounding tissues [4]-[6]. These low impedance points are thought to be the result of sensory and motor nerves emerging from deep tissue to superficial layers of the skin [7] and the change in impedance at acupuncture points is reported anywhere from between 1/2 to 1/20 of the impedance of the surrounding skin [8]-[9]. Small electrical potentials can be recorded on the skin at the terminal points of acupuncture meridians and the results are replicable under controlled experimental conditions [10]. As a result of these potentials, the current produced ranges from a few nA to several hundred nA, which can be recorded by an external measuring device. The electromotive force producing these endogenous currents results from electrical potentials at the acupuncture points on the skin and it is a function of the internal resistance of the point. Figure 1 shows the typical behaviour of the electrical resistance on an acupuncture point.

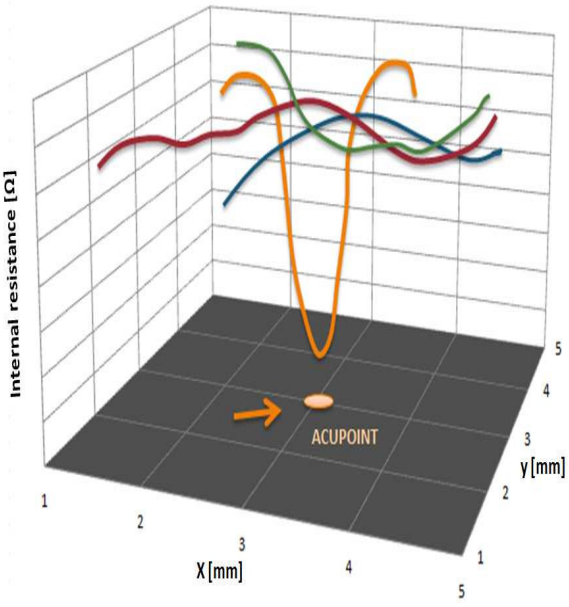

Figure 1: Electrical resistance of the acupuncture point.

The resistance is a function of the cutaneous region, skin humidity and pressure of the measurement electrode. The arrow in the figure highlights the strong decrease of resistance in the acupuncture point. The z coordinate reflects the resistance (Ω) and the x-y coordinates the movement of the electrode on the cutaneous surface (mm). In a previous work [11] a non-invasive probe was described, through which small electric currents can be measured at characteristic points on the skin in a replicable manner. The main purpose of the work presented here is the development of an effective graphical man-machine interface to facilitate the use of the non-invasive probe and to allow the correct evaluation of the measurements.

2. CURRENT MEASUREMENTS

A non-invasive probe was used to measure and record potentials and currents at the terminal points. Such a probe (shown in Figure 2) was designed to minimize all the main error components that may influence the measurements and makes it possible to perform repeatable and reliable measures. A 2 mm diameter silver/silver-chloride electrode was used as biomedical sensor [12]-[13]. A pressure compensation system was studied to allow the operator to push the probe on the measurement point to a well defined and constant pressure [14]. The presence of the pressure sensor allows the operator to work in a linear range of pressures in order to get the contact surface variation in a linear range too and to make the measurements almost insensitive to pressure changes for a wide span of values. Usually a span of 50-300g can be compensated. The status of the probe and of the pressure sensor can be checked anyway by the application software. It is also possible to modify the pressure compensation system parameters. Before performing any current acquisition the application software checks any possible residual pressure on the sensor.

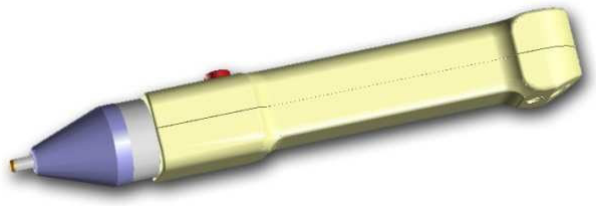

Figure 2: The used probe.

3. THE SOFTWARE TOOL

A Software Tool was designed to allow the optimal use of the probe and to show the results of the measurements. The following main steps have been followed:

1) *The general user and specific interface requirements for the probe and the pressure compensation system were determined;*

2) *An interface design which meets all the requirements previously determined was created and implemented;*

3) *The software tool was evaluated by a group of representative users and through a series of tests.*

The design effort resulted in a general purpose Software Tool that is highly adaptable and expandable. Figure 3 shows the Configuration Mask of the application, devoted to the initial set of parameters related to all instrument features. The mask allows the user to configure different kinds of current measurements, saving and displaying data in graphic or text formats and generating a report. A vocal synthesis system also provides an audio output of the results. In detail it is possible to configure:

- *The conditions for the acceptance of the measurements.*
  The tool calculates the standard deviation of the data in a given number of samples that can be set. When the standard deviation is lower than a pre-setable threshold, the current measure is accepted and displayed.

- *The pressure compensation parameters.*
  The user can modify the pressure compensation system parameters and check the status of the probe and of the pressure sensor. A patented algorithm was developed to set the minimum and maximum pressure level range and the absolute maximum upper and lower pressure limits for optimal compensation. If the maximum limits are exceeded, the measurement is aborted.

- *The voice synthesizer parameters.*
  Speech synthesis was implemented to improve the information capacity of the user. Many different types of information are provided to the user like suggesting where to place the probe, the name of the selected point and so on. All of this information can be very useful during operator training.

- *The on-line help.*
  The interactive help provides both text and speech answers. The operator can set the level of interaction required.

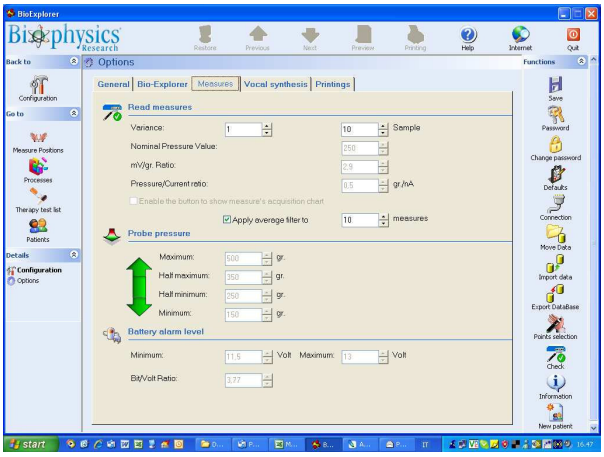

Figure 3: The Configuration Mask of the Software Tool.

The software package manages different kinds of current measurements, in a range of 30 to 3,000 nA, saving and displaying data in graphic or text formats (see Figure 4) and generating a printable report.

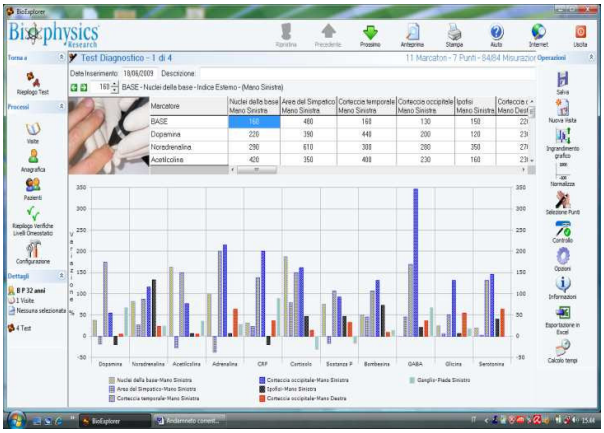

Figure 4: Displaying data in graphical and text formats.

All data either in text form or in graphics are stored in a data base together with all the information related to the test session. The measured current and the pressure exerted on the probe during the measurement can be displayed as a function of the time in a specific pattern (Figure 5). In order to minimize the measure error, the developed algorithm is able to automatically compensate the measure as a function of the pressure exerted on the probe. As can be seen in the figure, thanks to the action of the compensation algorithm, the current (red line) remains constant despite large variations in the pressure exerted on the probe (blue line).

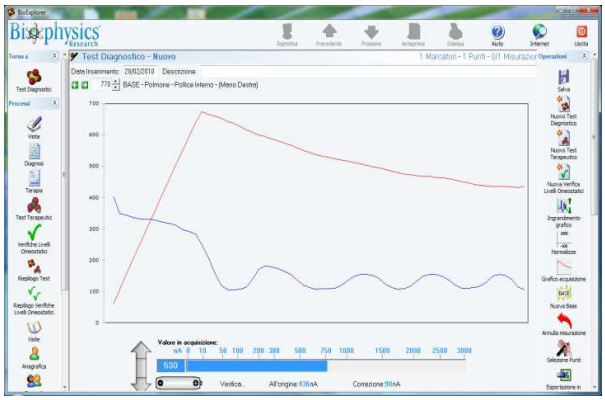

Figure 5: Displaying of the measured current and of the pressure exerted on the probe during the measurement.

4. RESULTS

The implementation combines a variety of graphical techniques to create a very powerful system and provide useful graphical results. The software uses a finite elements 3D model of the hand to visualize the measured currents along the characteristic points (Figure 6).

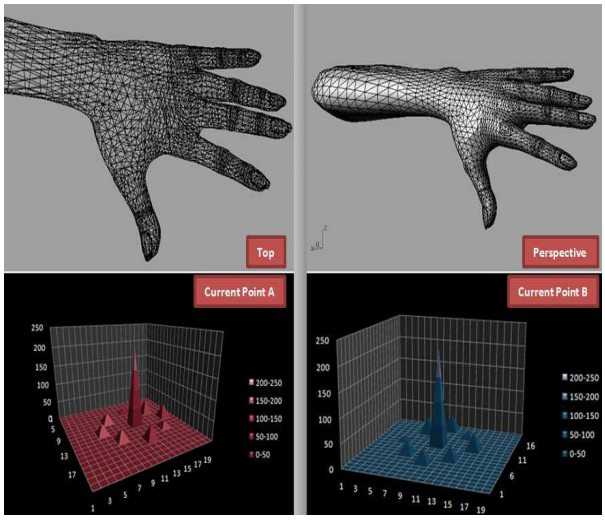

Figure 6: 3D visualization of the model of the hand and of the currents emitted by selected points.

Thanks to this model the points can be precisely identified on the surface of the skin together with the amplitudes of the measured currents. Figure 6 shows the Top and Perspective visualization of the 3D-model and of the currents emitted by selected points. The tool was used to test many characteristic points on different subjects and in particular to analyze points located at the hand. All the measurements were performed by holding the probe in an upright position, at an angle of 80 degrees to the skin, with the tip in contact with the characteristic point being tested. All the conducted measurements showed that the pressure compensation system allows the operator to work on the measurement point with a well defined and repetitive pressure obtaining reliable and repeatable measures that are virtually insensitive to fluctuations in pressure over a wide range of values. The pressure compensation system parameters can be checked and modified by the user through the Graphical User Interface. A computational unit calculates the standard deviation of the data coming from the acquisition circuit in a given number of samples. When the standard deviation is lower than a preset threshold, the current value is accepted and displayed in the results mask. To analyse the replicability of the measurements, the consistency of the currents emitted by different characteristic points over time for 10 minutes was studied.

N°	Current (nA)	Time (sec)	Standardized Current (p.u.)
1	320	0	0,9997
2	324	60	1,0122
3	312	120	0,9747
4	330	180	1,0309
5	315	240	0,9841
6	310	300	0,9684
7	312	360	0,9747
8	322	420	1,0059
9	324	480	1,0122
10	332	540	1,0372
MV	320,1		1
SD	7,69487564		

Table I: Results of measuring the currents emitted by point A 10 times.

Table I shows the results of measuring the currents emitted by point A 10 times with an interval of 60 seconds.

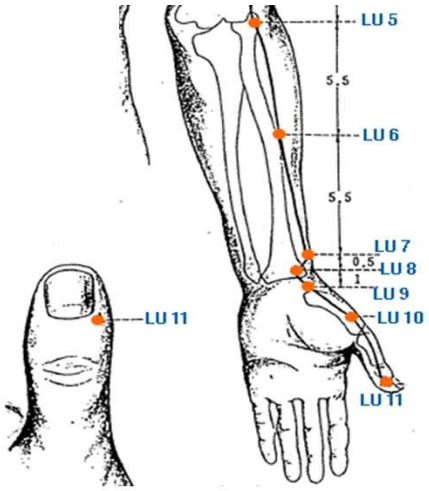

Figure 7: Various points along the Lung Channel.

Point A is point LU10 (Yu Ji or Fish Border) of the Lung Channel (see Figure 7) and is located in the depression behind the thenar eminence of the thumb, about the midpoint of the palmar side of the thumb, on the junction of the red and white skin. All the indicated currents are in nA and the table also provides the standard deviation (SD) and the mean value (MV). Figure 8 illustrates the standardized values of the current (in p.u.) showing that no significant change in current amplitude was found during the 10 minute period with regard to the point or its average value. The chart presents the mean value (MV) and the standard deviation (SD). Detectable currents were measured repeatedly at various point of the hand in different subjects at 60 sec intervals.

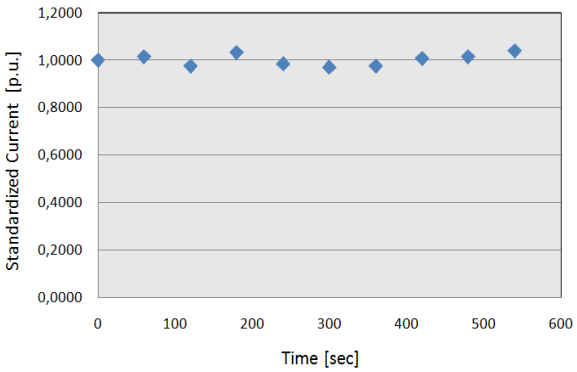

Figure 8: Standardized values of the currents emitted by point A every 60 seconds.

One of the innovative features of the tool is the possibility to create and visualize a 3D map of the characteristic points and of the related emitted currents. In fact it can be very useful to have a graphic representation of the value of the currents emitted by a characteristic point and by points located in the nearby surroundings. To perform these measurements the circular surface illustrated in Figure 9 was set.

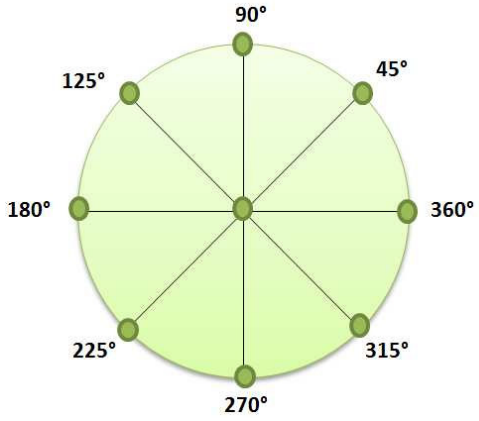

Figure 9: Map set to measure the currents emitted by points located in a 1cm radius circular area around the characteristic point.

This area is a 1cm radius circle and the centre of the circle represents the position of the point on the skin. The probe was first used to measure the current emitted by the characteristic point and then, moving the electrode around the circumference, to measure the currents emitted by points located at different angles. Detectable currents were measured repeatedly at a specific point of the hand in four different subjects. For example, Figure 10 shows the results of the current emitted by point LU-10 and by nearby points in the first subject. The figure shows the values of the currents emitted by the points in nA and the current % variation with regard to the value of the current emitted by the LU-10 point.

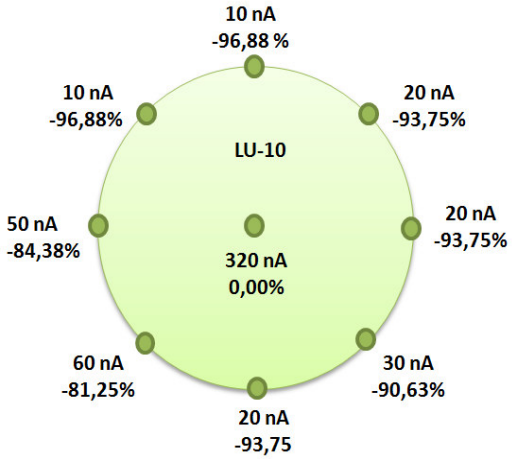

Figure 10: Values of the emitted currents and % variation.

Figure 11 shows the 3D graphical results of all the measured currents around point LU-10 and Figure 12 shows the current % variation with respect to the value measured in the characteristic point.

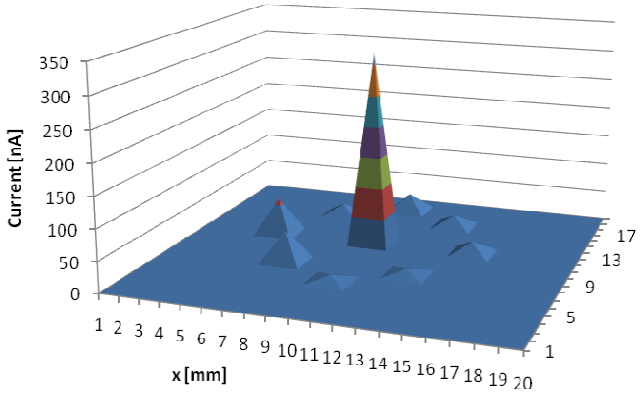

Figure 11: Visualization of the currents emitted by point LU-10 and nearby surrounding points in subject 1.

Figures 13 to 15 show the results of the currents emitted by point LU-10 and nearby surrounding points on the other 3 subjects. All 3D-graphics show the behaviour of the emitted currents in the 4 subjects indicating that the acupuncture points have higher emitted current than the nearby surrounding points. The results of the measurements can be displayed in a realistic way using the developed finite elements 3D model of the hand as illustrated in Figures 16-17. As can be seen in the figures, the model allows to exactly locate on the skin of the subject the points to be analyzed.

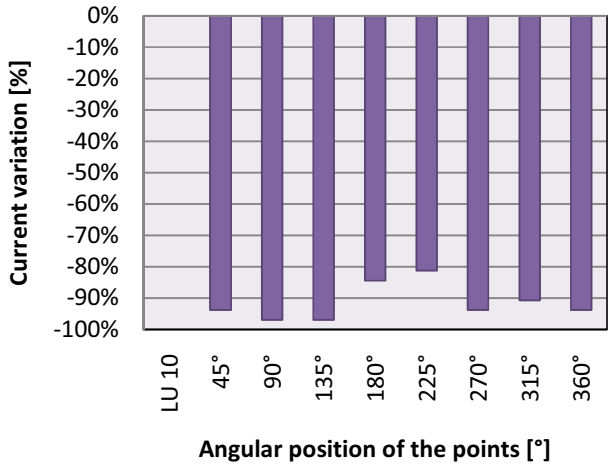

Figure 12: Current % variation respect to value measured in the characteristic point.

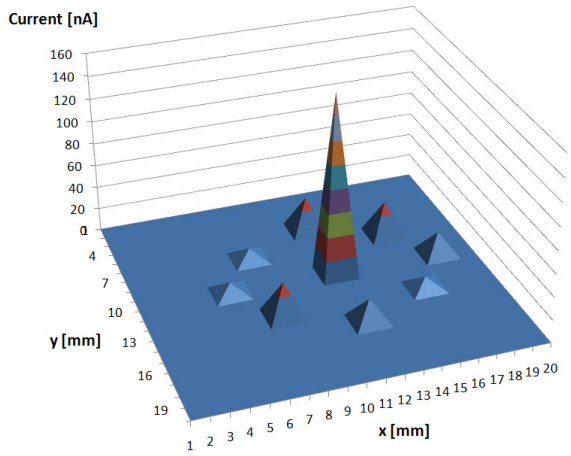

Figure 15: Visualization of the currents emitted by point LU-10 and nearby surrounding points in subject 4.

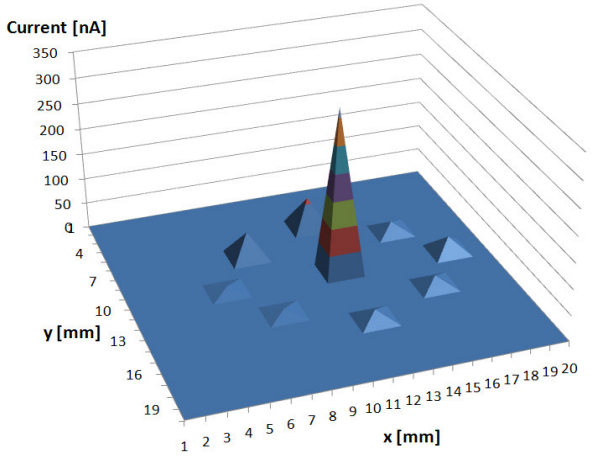

Figure 13: Visualization of the currents emitted by point LU-10 and nearby surrounding points in subject 2.

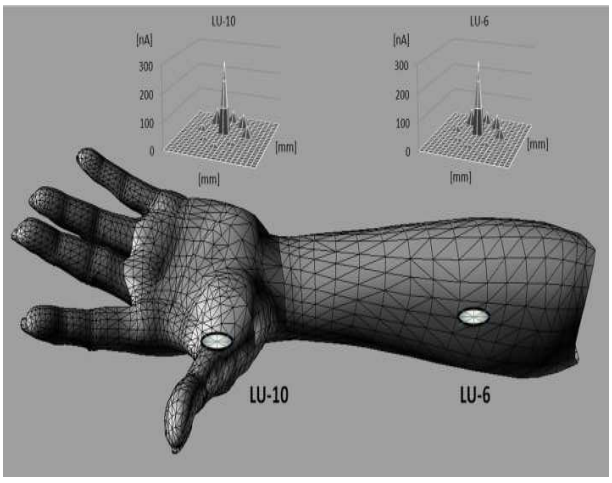

Figure 16: 3D model visualization of the currents emitted by characteristic points LU-10 and LU-6.

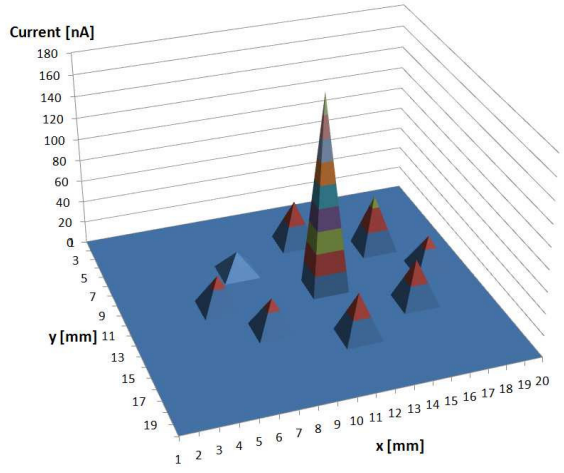

Figure 14: Visualization of the currents emitted by point LU-10 and nearby surrounding points in subject 3.

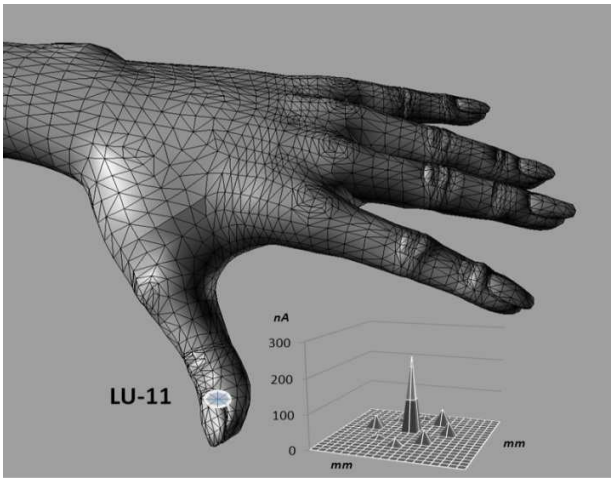

Figure 17: Visualization of the currents emitted by the characteristic point LU-11 of the hand.

Figure 18 shows the result of comparing the measurements effected on three characteristics points (LU-11, LU-10 and LU 6) along the Lung Channel of a male subject

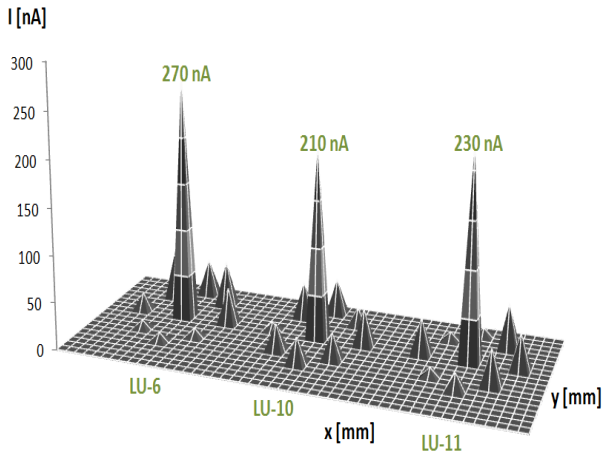

Figure 18: Visualization of the currents emitted by characteristic points of the lung channel LU-6, LU-10 and LU-11.

5. CONCLUSIONS

This work shows that small electric currents can be measured at characteristic points on the skin in a replicable manner with a non-invasive probe. In order to achieve a correct and meaningful evaluation of the magnitude of these currents, a probe and a software tool have been developed. The complete system (probe and tool) is versatile from the point of view of the hardware and software designs. The tool can be used to perform accurate and reliable analysis of the emitted currents and to easily go on to further applications and research in order to understand the correlation between any measureable point and the activity of the body organs. The tool provides different graphic representations of the results and a series of measurements have been presented and evaluated comparing the currents emitted by different characteristic points on the hands of a number of subjects.

6. ACKNOWLEDGEMENTS

This work was supported in part by the Portuguese Foundation for Science and Technology (FCT) under Project Nº SFRH/BPD/46224/2008 and Project Nº SFRH/BSAB/950/2009.

7. REFERENCES

[1] Z.X. Zhu, **Research advances in the electrical specificity of meridians and acupuncture points**, Am. J. Acupunct, N° 9, 1981, pp. 203-216.

[2] M. Reichmanis, A. Andrew, RO Becker, **Electrical correlates of acupuncture points**, IEEE Trans Biomed Eng, N° 22, 1975, pp. 533-535.

[3] M. Reichmanis, A. Andrew, R.O. Becker, **DC skin conductance variation at acupuncture points**, Am J Ch Med, N° 4, 1976, pp. 69-72.

[4] J..J. Tsuei, **The science of acupuncture**, IEEE Engineering in Medicine and Biology, May-June, 1996, pp. 52-57.

[5] K.G. Chen, **Electrical properties of meridians**, IEEE Engineering in Medicine and Biology, N° 15(3), 1996, pp. 58-63.

[6] G.D. Mc Carrol, B.A. Rowley, **An Investigation of the Existence of Electrically Located Acupuncture Points**, IEEE Transactions on Biomedical Engineering, Vol.BME-26, NO. 3, March 1979.

[7] H. Heine, **Manuale di Medicina Biologica**, Guna Editore, 1999, pp. 207-215, Milano (in italian).

[8] E.F. Prokhorov, J.G. Hernandez, Y.V. Vorobiev, E.M. Sinchez, T.E. Prokhorova, G. Zaldivar, **Electrophysical Characterization of Biologically Active Points and Human Skin by in Vivo Impedance Measurement**, Proceedings of the 22"d Annual EMBS International Conference, July 23-28, 2000, Chicago IL.

[9] W.A. Lu, J.J. Tsuei, K.G. Chen, **Preferential direction and symmetry of electric conduction of human meridians**, IEEE Eng. Med. Biol. Mag., 1999 vol. 18, p. 76.

[10] K.G. Chen, **Biological Implication of Electrical Properties of Acupuncture Meridians**, Proceedings of the 20th Annual International Conference of the IEEE Engineering in Medicine and Biology Society, Vol. 20, N° 2,1998, pp. 1086-1087.

[11] C.Boccaletti, F.Castrica, G.Fabbri, M.Santello, **A Non Invasive Biopotential Electrode for the Correct Detection of Bioelectrical Currents**, Proceedings of the Sixth IASTED International Conference on Biomedical Engineering, 2008, ISBN Hardcopy: 978-0-88986-721-5.

[12] R. Eickhorn, H. Schimmel, **Electrophysiological diagnosis at terminal poits of acupuncture meridians**, Biomedical Therapy, vol XVII, N° 3, 1999.

[13] M. O'Donnell, **Biomedical Instrumentation & Design**, BME/EECS 458, Chapter 3, Medical Instrumentation Application and Design (3rd Edition) John G. Webster Editor.

[14] G.Fabbri, C.Boccaletti, A. J. Marques Cardoso, F.Castrica, **A Bioelectrical Sensor for the Detection of Small Biological Currents**, Proceedings of The 4th International Conference on Sensing Technology, June 3-5, 2010, Lecce, Italy.